Hydrological Research Letters **10**(3), 81–87 (2016)
Published online in J-STAGE (www.jstage.jst.go.jp/browse/hrl). DOI: 10.3178/hrl.10.81

Effects of global warming on the impacts of Typhoon Mireille (1991) in the Kyushu and Tohoku regions

Tetsuya Takemi[1], Rui Ito[2] and Osamu Arakawa[3]
[1]*Disaster Prevention Research Institute, Kyoto University, Japan*
[2]*National Research Institute for Earth Science and Disaster Resilience, Japan*
[3]*Faculty of Life and Environmental Sciences, University of Tsukuba, Japan*

Abstract:

Typhoon Mireille (1991) caused devastation over Japan. Assessing the impacts of such an extreme typhoon under global warming is an important task to prevent and mitigate future natural disasters. This study investigated the influences of global warming on the strong winds of Typhoon Mireille by conducting pseudo-global warming (PGW) experiments with a regional model. Since significant damages to forest areas occurred in Kyushu and Tohoku, we compared the typhoon impacts in these two regions. It was demonstrated that on average the mean wind speeds induced by Typhoon Mireille become stronger in Kyushu and weaker in Tohoku under the PGW conditions than under the September 1991 conditions. The difference between the two regions in the future is due to the simulated typhoons under PGW being stronger at lower latitudes and weakening more rapidly at higher latitudes. Thus, the impacts of Typhoon Mireille under a warmed climate are considered to be more severe at a lower latitude and weaker at a higher latitude.

KEYWORDS typhoon; global warming; impact assessment; pseudo-global warming experiment

INTRODUCTION

Projecting changes in the intensity of tropical cyclones (TCs) under future global warming is an important issue, not only from a scientific point of view but also from the viewpoint of disaster impact assessment. Reflecting the significance of assessing typhoon disasters, a large number of studies have been conducted to investigate future changes in the structure, intensity, and impact of TCs, results of which can be found in the Fifth Assessment Report of the Intergovernmental Panel on Climate Change (IPCC) (IPCC, 2013, 2014).

For assessing TC impacts under global warming, there are several approaches. One is to simulate and project explicitly the global genesis of TCs in a general circulation model (GCM) at a high resolution that can resolve the overall structure of TCs (e.g., Murakami *et al.*, 2012). Regional climate models nested in GCMs can improve quantitative representations of TCs (Nakano *et al.*, 2010, 2012). The second approach is to estimate statistical characteristics by generating a large number of simulated typhoons with the assumption of a stochastic typhoon model, like the ones used in Fujii and Mitsuta (1986), Fujii (1998), and Nakajo *et al.* (2014). Another approach is to use a pseudo-global warming (PGW) experiment in which climate change components are added to past analysis fields in regional climate modeling (Sato *et al.*, 2007) to assess the impacts of climate change on the intensity of past extreme TCs. This study uses the PGW approach to investigate the influences of global warming on the change in regional-scale impacts of typhoons by examining the case of Typhoon Mireille (1991).

Typhoon Mireille (1991) developed on 16 September 1991 and intensified with its minimum central pressure being 925 hPa. The typhoon made landfall on the northern part of Kyushu, proceeded over the Sea of Japan, and landed again on Hokkaido. Owing to its track, Typhoon Mireille spawned widespread damages over urban and residential areas, agricultural areas, and forested areas in Japan (Mitsuta, 1992). This typhoon is locally known as "Apple Typhoon" because it caused significant damage to apple trees in the farmlands of northern Japan. Typhoon Mireille caused the most costly insurance loss among the tropical cyclones in the Pacific region during the period from 1970 to 2015 and is ranked 11th among all meteorological disasters during the same period (Swiss Reinsurance Company, 2016). In this respect, Typhoon Mireille is regarded as the worst typhoon during the past 45 years. A PGW experiment is useful to assess how the impacts of worst-case typhoons in the past change under a warmed climate (Mori and Takemi, 2016).

Although the intensity of tropical cyclones in the western North Pacific is projected to increase at their mature stage in a warmed climate (Murakami *et al.*, 2012), future changes in the impact of typhoons on Japan may depend on the geographical locations in question. Ito *et al.* (2016) indicated, by conducting PGW experiments, that the severity of Typhoon Songda (2004) in the northern part of Japan, i.e., Hokkaido, was reduced under warmed climate conditions, although the maximum intensity of the typhoon was strengthened. Thus, it is possible that an extreme typhoon, similar to Typhoon Songda, may have contrasting impacts in the southern and the northern part of Japan under global warming.

In this study, we investigate the influences of global warming on the strong winds of Typhoon Mireille (1991) in the Kyushu and Tohoku regions where significant damage to forests occurred. The impact assessment for forested areas is important because forests play a critical role in hydrological processes and the water cycle. For this purpose, PGW experiments and a simulation for reproducing the past event, similar to those in Ito *et al.* (2016), are conducted for Typhoon

Correspondence to: Tetsuya Takemi, Disaster Prevention Research Institute, Kyoto University, Gokasho, Uji, Kyoto 611-0011, Japan. E-mail: takemi@storm.dpri.kyoto-u.ac.jp

Received 9 August, 2016
Accepted 13 October, 2016
Published online 12 November, 2016

Mireille. Because the tracks of Mireille and Songda are similar, the robustness of the finding in Ito *et al.* (2016) is expected to be increased.

NUMERICAL MODEL AND EXPERIMENTAL SETTINGS

The numerical model used here is the Weather Research and Forecasting (WRF) model/the Advanced Research WRF (ARW) version 3.6.1 (Skamarock *et al.*, 2008). Two-way nesting capability was used to cover the western North Pacific region including the Japanese islands in the outermost domain at a coarser resolution and to resolve complex terrain features in the finest-resolution nested domains, because the representation of topography is important in reproducing strong winds in complex terrain (Takemi, 2009; Oku *et al.*, 2010). Figure 1 shows the computational domains. Domain 1, the outermost domain, had a 9-km grid spacing, while the nested domain, Domain 2, had a 3-km grid. Domain 2 had two nested domains, Domain 3 at a 1-km grid, covering the Kyushu and Tohoku regions, separately. All the domains had 57 vertical levels, and the model top was set to be 20 hPa. The parameterizations for physical processes were chosen in the same way as used in Ito *et al.* (2016).

For the initial and boundary conditions of the WRF model, we used a 6-hourly, 1.25°-resolution long-term reanalysis dataset from the Japanese 55-year Reanalysis (JRA-55) (Kobayashi *et al.*, 2015). The spectral nudging technique of the WRF model was employed to incorporate the synoptic-scale influences on the simulated typhoons. In addition, the TC bogus scheme was used to initialize the TC vortex, based on the best-track data of the Regional Specialized Meteorological Center (RSMC) in Tokyo. The options for spectral nudging and the TC bogus scheme are the same as those used in Ito *et al.* (2016). The initial time for time integration was 1200 UTC 25 September 1991. This historical run is referred to as CNTL.

In order to perform PGW experiments, we used simulated data from MRI-AGCM version 3.2 at a 20-km resolution (Mizuta *et al.*, 2012) for the present climate (corresponding to the period of 1979–2003) and future climates under the Representative Concentration Pathway (RCP)-8.5 scenario (corresponding to the period of 2075–2099). The projection data for future climates consisted of those driven by four different sea surface temperature (SST) patterns: the ensemble mean SST pattern from the CMIP5 atmosphere-ocean coupled models and the three SST patterns obtained by cluster analysis for the CMIP5 model outputs (Clusters 1, 2, and 3) (Mizuta *et al.*, 2014). For each meteorological variable, warming increments were defined as the difference in the monthly means of the future climate from the present climate. As we were examining Typhoon Mireille, we used the monthly incremental data for September.

In the PGW experiments, we did not add relative humidity and wind as warming increments, based on the consideration that relative humidity has no significant change from the present to the future climate (Takemi *et al.*, 2012) and wind has significant effect on the typhoon track. With these common settings, 6 cases were examined as PGW experiments. One case was to add surface variables including SST, surface air temperature, and surface pressure, and three-dimensional geopotential and temperature as the warming increments (referred to as PGW1). The second was to add SST, surface air temperature, and three-dimensional temperature as the warming increments (PGW2). As an extreme case, the third was to add only the SST increment (PGW3). We also conducted three other experiments with fully added increments (except relative humidity and wind) from the AGCM runs with three SST clusters (referred to as PGWC1 for SST Cluster 1, PGWC2 for SST Cluster 2, and PGWC3 for SST Cluster 3). The incremental data used here are exactly the same as in Ito *et al.* (2016). The spatial distributions of the increments can be found in Ito *et al.* (2016).

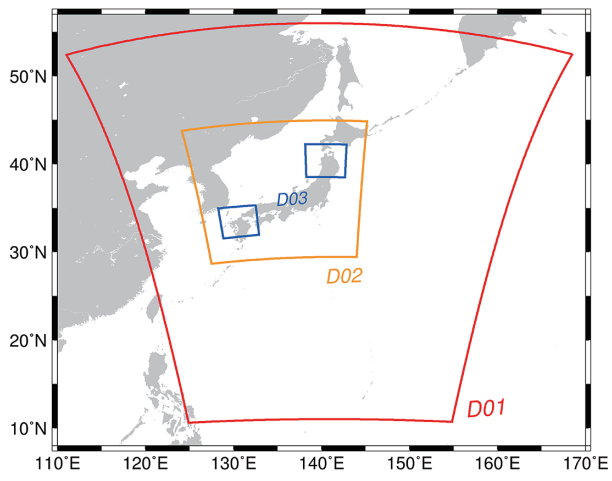

Figure 1. The computational domains: Domain 1 (D01) at 9-km grid, Domain 2 (D02) at 3-km grid, and Domain 3 (D03) (covering separate areas of Kyushu and Tohoku) at 1-km grid

RESULTS

In the following analyses, the simulated outputs from the 1-km domains are used.

First, the overall performance of the model simulations is compared with the best-track data in terms of the typhoon track and the surface pressure at the typhoon center. Figure 2a shows the tracks of the typhoons in the best-track data and in the simulations. It is seen that the CNTL simulation for reproducing Typhoon Mireille (1991) successfully captures the observed track from the south to the north. The simulated typhoons in the PGW experiments also take tracks similar to the observation and to CNTL. Considering that the typhoon tracks significantly affect local-scale strong winds and rainfall (Oku *et al.*, 2014; Mori *et al.*, 2014; Takayabu *et al.*, 2015; Mori and Takemi, 2016), the agreement of the simulated TC tracks with the observation is a first priority in assessing the impacts of typhoons. In this sense, the favorable agreement of the simulated tracks between the CNTL and the PGW experiments should give credence to the following analyses.

Figure 2b compares the temporal change of the typhoon intensity in CNTL with the best-track. Intensification on 26 September, rapid weakening on 27 September, and re-intensification on 28 September seen in the best-track are

well reproduced in CNTL. In the PGW experiments, a similar tendency is seen, but quantitatively the intensity and the intensity change are quite different. Compared with the CNTL result, the typhoons in the PGW experiments are more intensified on 26 September, weaken more rapidly on 27 September, and re-intensify slightly stronger on 28 September. Note that the re-intensification phase on 28 September corresponds to the period when the typhoons make landfall on Hokkaido. This result is in contrast to that seen in the PGW experiments for Typhoon Songda (2004) examined by Ito *et al.* (2016) who showed that the typhoons under PGW conditions are weaker than that under the September 2004 condition at the re-intensification stage. This point will be discussed later in this section.

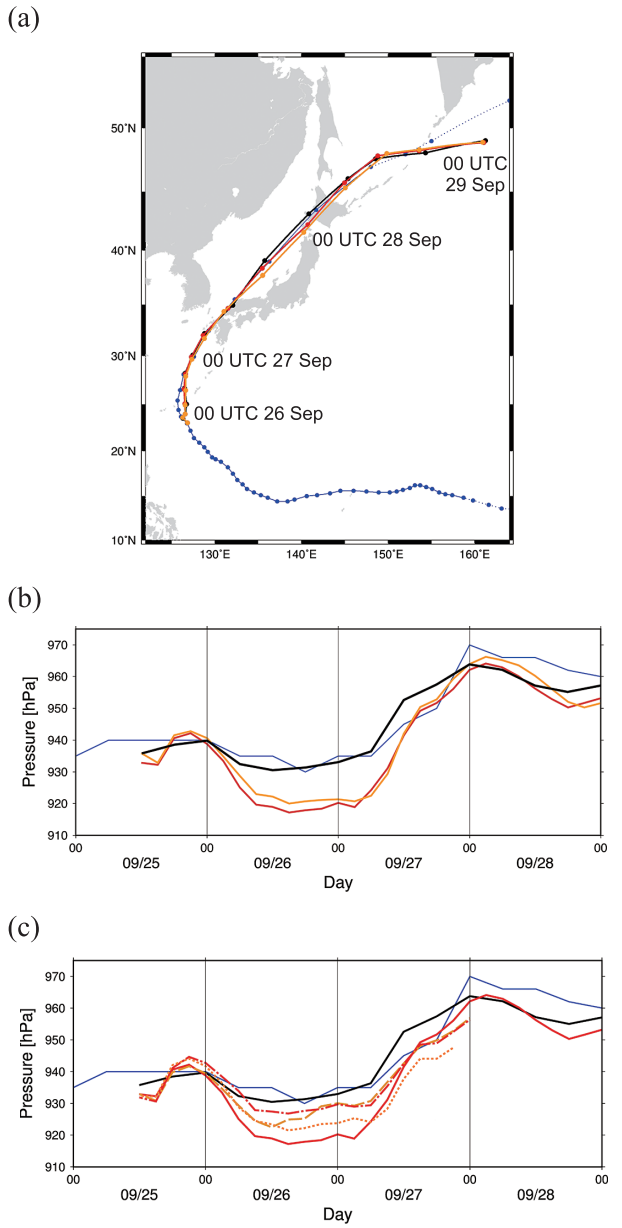

Figure 2. The comparison between the RSMC (Regional Specialized Meteorological Center) best-track of Typhoon Mireille (1991) (blue solid line) and the simulated typhoons (CNTL: black solid, PGW1: red solid, PGW2: orange solid; PGWC1: red dash-dotted, PGWC2: orange dashed, PGWC3: orange dotted). (a) The observed track and the simulated track, and the time series of central surface pressure for (b) the best-track, CNTL, PGW1, and PGW2, and for (c) the best-track, CNTL, PGW1, PGWC1, PGWC2, and PGWC3

With the use of the 20-km-resolution AGCM ensemble runs with SST Clusters 1, 2, and 3, we conducted another PGW experiments to examine whether the intensification and rapid weakening seen in PGW1 and PGW2 is robust. In Figure 2c, the time series of the central pressure in PGWC1, PGWC2, and PGWC3 are compared with those in PGW1 as well as the best-track and CNTL. Although the maximum intensities in PGWC1, PGWC2, and PGWC3 are weaker than that in PGW1, the simulated typhoons in all the PGW experiments are more intensified at their maturity and weakened more rapidly than that in CNTL. Thus, the feature of the intensity change seems to be robust irrespective of the AGCM runs with different SST patterns prescribed.

Table I summarizes the minimum central surface pressure during the lifetime of the typhoons in the best track and in the simulations. The simulated typhoons all intensify under the PGW climate compared to the actual condition in September 1991. The extreme condition with only warmed SST prescribed (PGW3) produced an extreme typhoon with a minimum pressure of 887 hPa. The present result of stronger TCs under global warming is consistent with the cases of Typhoon Vera (1959) (Mori and Takemi, 2016), Typhoon Haiyan (2013) (Takayabu *et al.*, 2015), and Typhoon Songda (2004) (Ito *et al.*, 2016), and previous studies with GCMs (e.g., Murakami *et al.*, 2012). Based on these results, we examine the differences between the CNTL and PGW experiments in the followings.

Figure 3 demonstrates the spatial distribution of mean surface wind speeds in CNTL, PGW1, and PGW2 and their differences from the CNTL to the PGW conditions in the Kyushu region of D03 (Figure 1). The mean surface wind speed is computed at the 10-m height above the ground level and is averaged over time during the period between 0000 UTC 27 and 0000 UTC 29 September. In CNTL (Figure 3a), stronger winds widely spread in the domain, specifically in the coastal areas, the mountainous areas in the middle of Kyushu, and the westernmost areas and the mountainous areas in the Honshu Island. Comparison of the results in CNTL with the surface observations indicates that the simulations mostly overestimate the mean wind speed. In general, quantitative representation of surface winds in numerical simulations is not easy owing to some issues: the observed wind speed is a 10-minute mean value and is hence weaker than the wind over shorter timescales; the observation points are affected by surrounding topography and buildings; and

Table I. Minimum surface central pressure during the typhoon lifetime of the best-track (OBS) and the simulated cases

Case	OBS	CNTL	PGW1	PGW2	PGW3	PGWC1	PGWC2	PGWC3
Pressure (hPa)	930	931	917	920	887	923	928	922

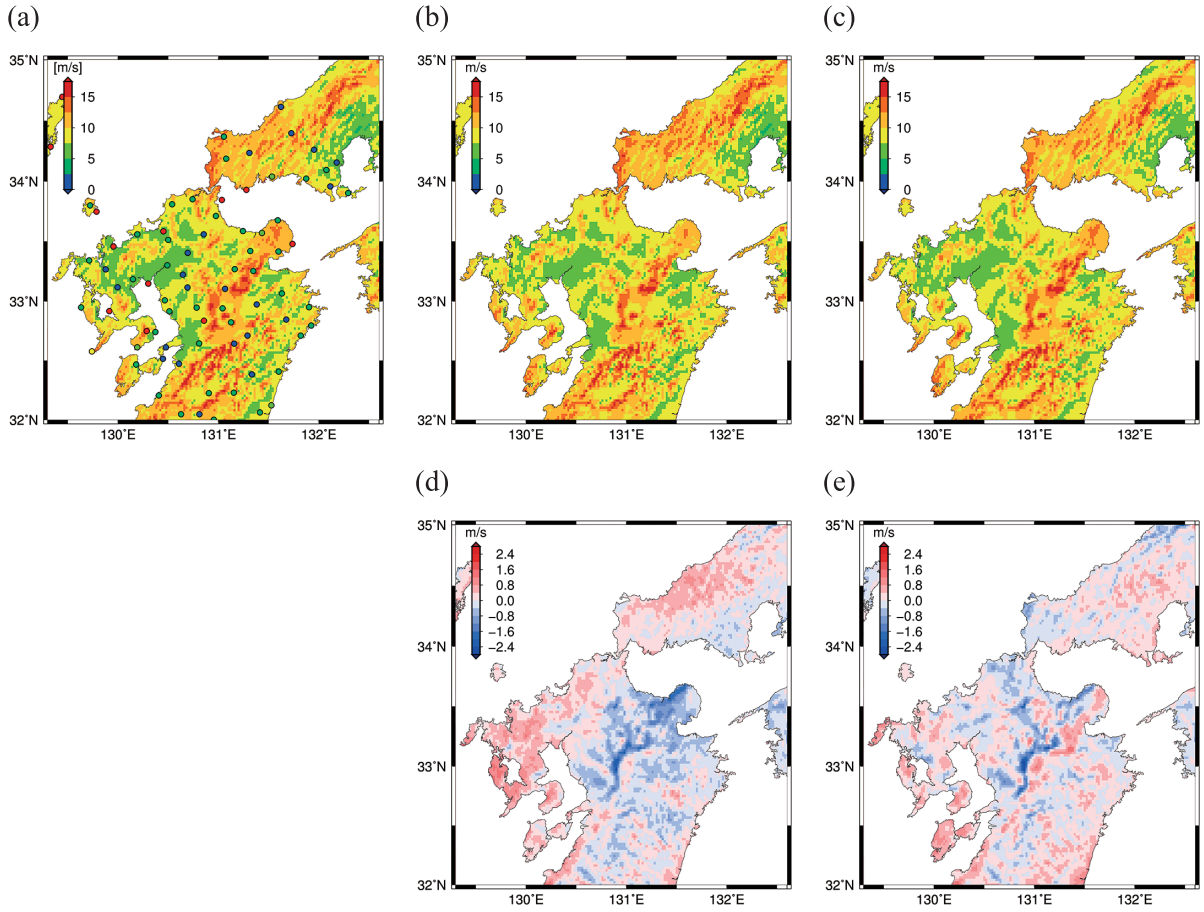

Figure 3. The spatial distribution of temporal-mean surface wind speed averaged during the simulated period from 0000 UTC 27 to 0000 UTC 29 September for (a) CNTL, (b) PGW1, and (c) PGW2 in the Kyushu region. The observed mean wind speeds at the AMeDAS stations during the same period are denoted by colored circles. The difference of the mean wind speed of (d) PGW1 minus CNTL and (e) PGW2 minus CNTL

the model does not incorporate surface roughness characteristics precisely. It is considered that similar issues also appear in the present simulation. More discussion on Figure 3a is given in Supplement Text S1.

The spatial distributions of the mean wind speeds in PGW1 and PGW2 are shown in Figures 3b and 3c, and the differences of the mean wind speeds in the PGW cases minus CNTL are indicated in Figures 3d and 3e. The spatial patterns of stronger wind in the PGW cases appear to be similar to those in CNTL. Taking the differences between the CNTL and the PGW experiments demonstrates that there are areas with increased or decreased wind speeds in PGW1 and PGW2 from CNTL. Common features can be found for increased wind speed under the PGW conditions in coastal areas in the northwestern to western part and in the Pacific side of Kyushu. In contrast, there are fine-scale patterns with increased/decreased winds in the mountainous areas in the middle of Kyushu. Such patterns suggest that the changes in wind speeds in in-land areas are more complex than those in coastal areas, probably owing to topographical influences. The mean differences averaged over the land grids in the domain are $+0.03\ \mathrm{m\ s^{-1}}$ for PGW1 minus CNTL and $+0.07\ \mathrm{m\ s^{-1}}$ for PGW2 minus CNTL, indicating that the wind speed averaged over the period, including the approach and landfall of the typhoon, is enhanced in the PGW experiments.

The spatial distributions of the mean wind speeds in CNTL, PGW1, and PGW2 as well as their differences between CNTL and PGW1 (or PGW2) for the Tohoku region is shown in Figure 4. Similar to the feature found in Figure 3a, comparison of the simulated wind speed in CNTL with the surface observations (Figure 4a) indicates that the simulation in general overestimates the wind speed. Stronger wind speeds are seen on the coastal areas of the Sea of Japan side and in the mountainous areas in the center and the eastern part of the Tohoku region, while winds are weaker in the in-land areas surrounded by mountains. See further discussion in Supplement Text S1. Similar spatial patterns in wind speed can be seen in the PGW1 and PGW2 results (Figures 4b and 4c).

Similar to the analysis for Kyushu, the differences in the mean wind speeds between CNTL and the PGW experiments for the Tohoku region are examined. Figures 4d and 4e demonstrate the spatial distributions of the differences in Tohoku. In this case negative values seem to be more widespread across the region than in the Kyushu case. A decrease on the coastal areas facing westward appears to be pronounced, and enhanced decrease can also be found in some in-land areas and in the eastern part of Tohoku. There are some areas of increased wind speeds in the middle of

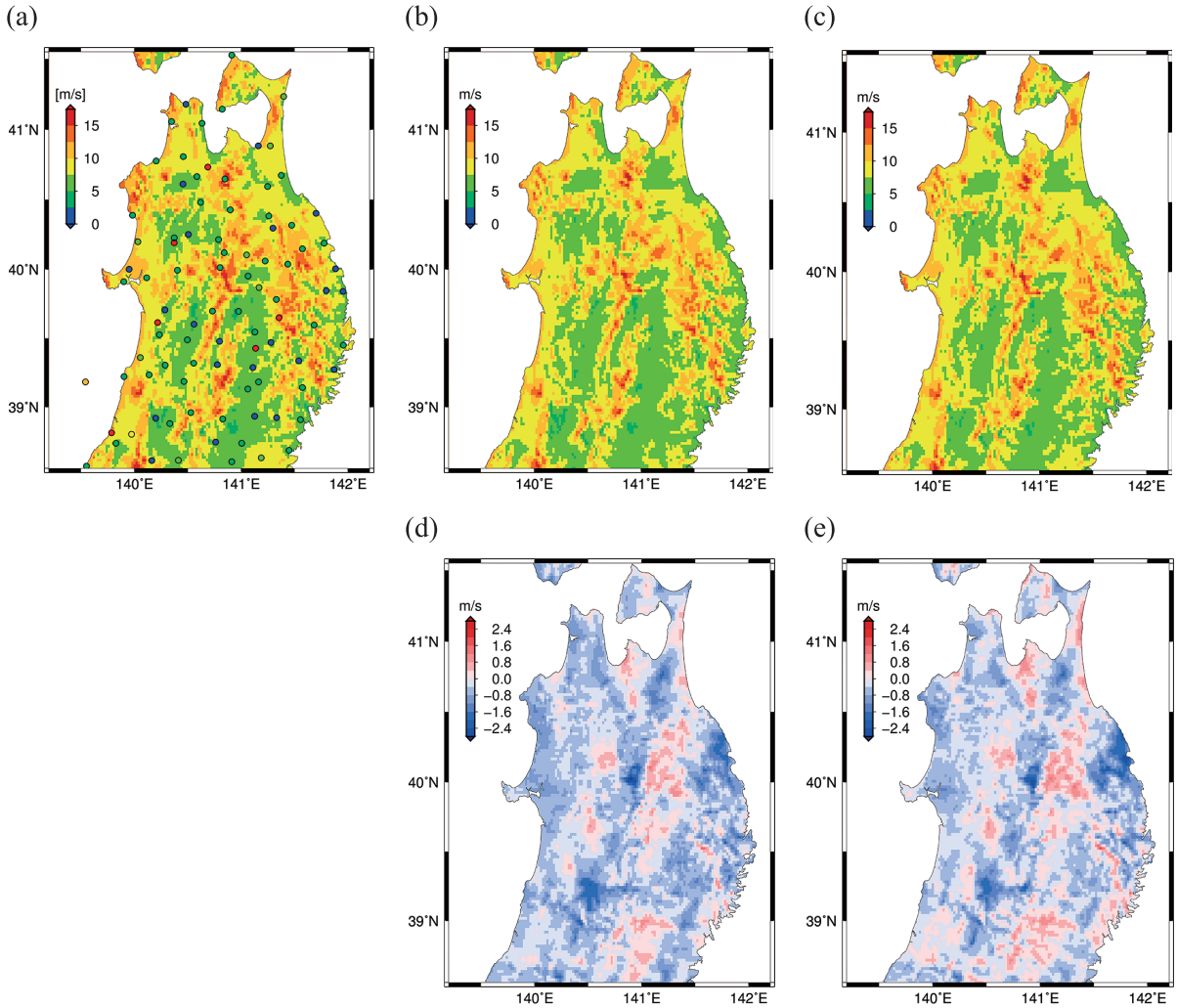

Figure 4. The same as Figure 3, except for the Tohoku region

Tohoku. As a whole, the domain-mean difference of the mean wind speed over the land grids between CNTL and PGW1 (PGW2) is –0.4 (–0.3) m s^{-1}. The negative differences mean that averaged winds during the typhoon passage over the Tohoku region become weaker under the PGW conditions than under the actual September 1991 conditions.

Comparing the results demonstrated in Figures 3d/3e and 4d/4e suggests that the impacts of an extreme typhoon like Typhoon Mireille (1991) depend on the geographical location over the Japanese islands. To explain this, we revisit the case study of Typhoon Songda (2004) in Ito *et al.* (2016): it was found that typhoon winds over the Hokkaido region became weaker under the PGW conditions than under the actual conditions. Owing to enhanced warming at higher latitudes under the PGW conditions, baroclinicity decreased, which negatively affected re-intensification of the typhoon during extra-tropical transition and therefore made the typhoon weaker during the re-intensification phase. Here we also examined the meridional gradient of potential temperature for the Mireille case and found that baroclinicity was slightly decreased over the Sea of Japan off the Tohoku coast and over the Hokkaido region in the PGW experiments, although the magnitude of the decreased baroclinicity was smaller in the Mireille case than in the Songda case (not shown). This decreased baroclinicity is considered to influence more rapidly weakening typhoons in PGW1 and PGW2 and slightly weaker typhoons in PGW1 and PGW2 just after 0000 UTC 28 September than the simulated typhoon in CNTL. On 28 September, the typhoon made landfall on Hokkaido. Among the three regions (Kyushu, Tohoku, and Hokkaido), Kyushu, located at the southernmost latitude, experienced stronger winds due to Typhoon Mireille under a warmed climate than in the actual case, and Tohoku, located in northern Japan and just to the south of Hokkaido, experienced weaker winds under a warmed climate. Therefore, the impacts of Typhoon Mireille under warmed climate conditions are considered to be more severe at lower latitudes and weaker at higher latitudes.

One point to note here is that in assessing disaster impacts from a typhoon maximum wind speeds during typhoon passage should also be taken into consideration. Figure 5 compares the mean and the maximum wind speeds during the simulated period in CNTL and PGW2 at the land grids in the Kyushu and Tohoku regions. Corresponding to the results shown in Figures 3 and 4, it is seen that the mean wind speed is stronger (weaker) in Kyushu (Tohoku) in PGW2 than in CNTL. However, the maximum wind speed is stronger in both regions in PGW2. See Supplement Figures S2 and S3

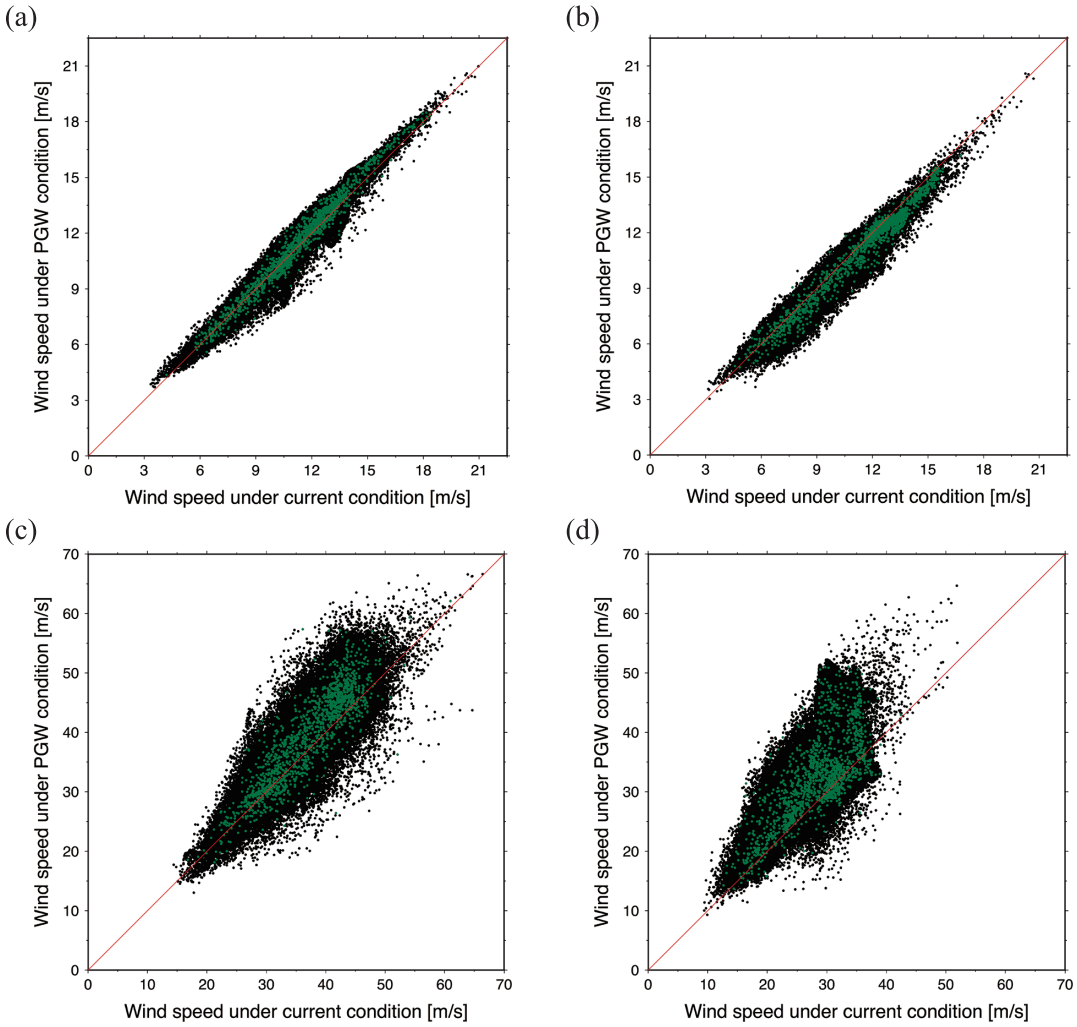

Figure 5. Scatter diagram of the mean wind speed between CNTL and PGW2 averaged during the simulated period at the land grids in (a) the Kyushu region and (b) the Tohoku region. Scatter diagram of the maximum wind speed between CNTL and PGW2 during the simulated period in (c) Kyushu and (d) Tohoku. The black dots indicate all the land grids in each region, while the green dots indicate grids thinned at the 0.1 degree interval in each region

for the spatial distribution of the maximum wind speed in Kyushu and Tohoku. The stronger maximum wind in Tohoku in PGW2 may partly be due to the simulated track in PGW2 being slightly shifted eastward from that in CNTL (see Figure 2a), generating stronger winds in Tohoku. In the present simulation technique, it is quite difficult to completely regulate the typhoon track, and slight changes cannot be avoided depending on the simulations. More precise techniques should be employed in future analyses. Furthermore, there may be other physical mechanisms to explain the stronger maximum winds under PGW conditions. More detailed analyses on the structural changes of extreme typhoons at higher latitudes are required in future studies.

CONCLUSIONS

By conducting PGW experiments, we have investigated the influences of global warming on the strong winds of Typhoon Mireille (1991) and showed that typhoon impacts under global warming differ depending on the latitude of the region of interest. Since significant damage to forested areas occurred in the Kyushu and Tohoku regions, we have compared the typhoon impacts in these two regions.

On average the mean wind speeds induced by Typhoon Mireille become stronger in Kyushu and weaker in Tohoku under the PGW future climates than under the September 1991 conditions. Future differences between the two regions are due to the simulated typhoons being stronger at lower latitudes in PGW than in CNTL and weakening more rapidly at higher latitudes in PGW. The impacts of Typhoon Mireille under warmed climate conditions is considered to be more severe at a lower latitude and weaker at a higher latitude.

Forested area covers about two-thirds of the total Japanese land area. Preserving forests in the future may depend on the assessment of changes in typhoon impacts under global warming. Continuous efforts should be made to investigate various types of typhoons.

ACKNOWLEDGMENTS

This work was conducted under the framework of the Program for Risk Information on Climate Change (SOUSEI) supported by Ministry of Education, Culture, Sports, Science and Technology, Japan, and was also supported by JSPS Kakenhi 16H01846.

SUPPLEMENTS

Text S1. Additional explanation on the distributions of wind speed shown in Figures 3a and 4a

Figure S1. Land-use categories used for the WRF model in the Domain 3 regions of Kyushu and Tohoku

Figure S2. The same as Figure 3, except for the maximum wind speed during the simulated period

Figure S3. The same as Figure 4, except for the maximum wind speed during the simulated period

REFERENCES

Fujii T. 1998. Statistical analysis of the characteristics of severe typhoons hitting the Japanese main islands. *Monthly Weather Review* **126**: 1091–1097. DOI: 10.1175/1520-0493(1998)126<1091:SAOTCO>2.0.CO;2.

Fujii T, Mitsuta Y. 1986. Synthesis of a stochastic typhoon model and simulation of typhoon winds. *Annuals of Disaster Prevention Research Institute, Kyoto University* **29B1**: 229–240.

IPCC. 2013. Climate Change 2013: The Physical Science Basis. Contribution of Working Group I to the Fifth Assessment Report of the Intergovernmental Panel on Climate Change. Cambridge University Press, Cambridge, UK and New York, NY, USA; 1535.

IPCC. 2014. Climate Change 2014: Impacts, Adaptation, and Vulnerability. Part A: Global and Sectoral Aspects. Contribution of Working Group II to the Fifth Assessment Report of the Intergovernmental Panel on Climate Change. Cambridge University Press, Cambridge, UK and New York, NY, USA; 1132.

Ito R, Takemi T, Arakawa O. 2016. A possible reduction in the severity of typhoon wind in the northern part of Japan under global warming: A case study. *SOLA* **12**: 100–105. DOI: 10.2151/sola.2016-023.

Kobayashi S, Ota Y, Harada Y, Ebita A, Moriya M, Onoda H, Onogi K, Kamahori H, Kobayashi C, Endo H, Miyaoka K, Takahashi K. 2015. The JRA-55 Reanalysis: General specifications and basic characteristics. *Journal of the Meteorological Society of Japan* **93**: 5–48. DOI: 10.2151/jmsj.2015-001.

Mitsuta Y. 1992. Studies on Strong Wind Disasters Induced by Typhoon Number 19 in 1991 (Mireille). Report of Urgent Investigation on Natural Disasters, Ministry of Education Scientific Research, Japan; 369 (in Japanese).

Mizuta R, Yoshimura H, Murakami H, Matsueda M, Endo H, Ose T, Kamiguchi K, Hosaka M, Sugi M, Yukimoto S, Kusunoki S, Kitoh A. 2012. Climate simulations using MRI-AGCM3.2 with 20-km grid. *Journal of the Meteorological Society of Japan* **90A**: 233–258. DOI: 10.2151/jmsj.2012-A12.

Mizuta R, Arakawa O, Ose T, Kusunoki S, Endo H, Kitoh A. 2014. Classification of CMIP5 future climate responses by the tropical sea surface temperature changes. *SOLA* **10**: 167–171. DOI: 10.2151/sola.2014-035.

Mori N, Takemi T. 2016. Impact assessment of coastal hazards due to future changes of tropical cyclones in the North Pacific Ocean. *Weather and Climate Extremes* **11**: 53–69. DOI: 10.1016/j.wace.2015.09.002.

Mori N, Kato M, Kim S, Mase H, Shibutani Y, Takemi T, Tsuboki K, Yasuda T. 2014. Local amplification of storm surge by Super Typhoon Haiyan in Leyte Gulf. *Geophysical Research Letters* **41**: 5106–5113. DOI: 10.1002/2014GL060689.

Murakami H, Wang Y, Yoshimura H, Mizuta R, Sugi M, Shindo E, Adachi Y, Yukimoto S, Hosaka M, Kusunoki S, Ose T, Kitoh A. 2012. Future changes in tropical cyclone activity projected by the new high-resolution MRI-AGCM. *Journal of Climate* **25**: 3237–3260. DOI: 10.1175/JCLI-D-11-00415.1.

Nakajo S, Mori N, Yasuda T, Mase H. 2014. Global stochastic tropical cyclone model based on principal component analysis with cluster analysis. *Journal of Applied Meteorology and Climatology* **53**: 1547–1577. DOI: 10.1175/JAMC-D-13-08.1.

Nakano M, Kanada S, Kato T. 2010. Statistical analysis of simulated direct and indirect precipitation associated with typhoons around Japan using a cloud-system resolving model. *Hydrological Research Letters* **4**: 6–10. DOI: 10.3178/hrl.4.6.

Nakano M, Kato T, Hayashi S, Kanada S, Yamada Y, Kurihara K. 2012. Development of a 5-km-mesh cloud-system-resolving regional climate model at the Meteorological Research Institute. *Journal of the Meteorological Society of Japan* **90A**: 339–350. DOI: 10.2151/jmsj.2012-A19.

Oku Y, Takemi T, Ishikawa H, Kanada S, Nakano M. 2010. Representation of extreme weather during a typhoon landfall in regional meteorological simulations: A model intercomparison study for Typhoon Songda (2004). *Hydrological Research Letters* **4**: 1–5. DOI: 10.3178/hrl.4.1.

Oku Y, Yoshino J, Takemi T, Ishikawa H. 2014. Assessment of heavy rainfall-induced disaster potential based on an ensemble simulation of Typhoon Talas (2011) with controlled track and intensity. *Natural Hazards and Earth System Sciences* **14**: 2699–2709. DOI: 10.5194/nhess-14-2699-2014.

Sato T, Kimura F, Kitoh A. 2007. Projection of global warming onto regional precipitation over Mongolia using a regional climate model. *Journal of Hydrology* **333**: 144–154. DOI: 10.1016/j.jhydrol.2006.07.023.

Skamarock WC, Klemp JB, Dudhia J, Gill DO, Barker DM, Duda MG, Huang XY, Wang W, Powers JG. 2008. A description of the Advanced Research WRF version 3. *NCAR Technical Note*, NCAR/TN-47 + STR; 113.

Swiss Reinsurance Company. 2016. Natural Catastrophes and Man-Made Disasters in 2015: Asia Suffers Substantial Losses. Swiss Re Sigma Reports, Switzerland; 47.

Takayabu I, Hibino K, Sasaki H, Shiogama H, Mori N, Shibutani Y, Takemi T. 2015. Climate change effects on the worst-case storm surge: A case study of Typhoon Haiyan. *Environmental Research Letters* **10**: 064011. DOI: 10.1088/1748-9326/10/6/064011.

Takemi T. 2009. High-resolution numerical simulations of surface wind variability by resolving small-scale terrain features. *Theoretical and Applied Mechanics Japan* **57**: 421–428. DOI: 10.11345/nctam.57.421.

Takemi T, Nomura S, Oku Y, Ishikawa H. 2012. A regional-scale evaluation of changes in environmental stability for summertime afternoon precipitation under global warming from super-high-resolution GCM simulations: A study for the case in the Kanto Plain. *Journal of the Meteorological Society of Japan* **90A**: 189–212. DOI: 10.2151/jmsj.2012-A10.